NFFT based fast Ewald summation for various types of periodic boundary conditions

Franziska Nestler, Michael Pippig and Daniel Potts

Technische Universität Chemnitz
Faculty of Mathematics
09107 Chemnitz, Germany
E-mail: {franziska.nestler, michael.pippig, daniel.potts}@mathematik.tu-chemnitz.de

The fast calculation of long-range interactions is a demanding problem in particle simulation. In this tutorial we present fast Fourier-based methods for the Coulomb problem with mixed periodicity. The main focus of our approach is the decomposition of the problem into building blocks that can be efficiently realized. For that reason we recapitulate the fast Fourier transform at nonequispaced nodes (NFFT) and the fast summation method. Application of these two methods to the Ewald splitting formulas yields efficient methods for calculating the Coulomb energies in 3d-periodic, 2d-periodic, 1d-periodic, and also in 0d-periodic (open) boundary conditions.

1 Introduction

We start with a formal definition of the Coulomb problem with mixed periodic boundary conditions. Assume that N charges $q_j \in \mathbb{R}$ at positions $\boldsymbol{x}_j \in \mathbb{R}^3$, $j = 1, \ldots, N$, fulfill the charge neutrality condition

$$\sum_{j=1}^{N} q_j = 0. \tag{1.1}$$

The total Coulomb energy of the particle system can be formally written as

$$U_{\mathcal{S}} := \frac{1}{2} \sum_{j=1}^{N} q_j \phi_{\mathcal{S}}(\boldsymbol{x}_j),$$

where for each particle j the potential $\phi_{\mathcal{S}}(\boldsymbol{x}_j)$ is given by

$$\phi_{\mathcal{S}}(\boldsymbol{x}_j) := \sum_{\boldsymbol{n} \in \mathcal{S}} \sum_{i=1}^{N}{}' \frac{q_i}{\|\boldsymbol{x}_{ij} + L\boldsymbol{n}\|}. \tag{1.2}$$

Thereby, we denote by $\| \cdot \|$ the Euclidean norm and define the difference vectors $\boldsymbol{x}_{ij} := \boldsymbol{x}_i - \boldsymbol{x}_j$. The edge length of the simulation box in each dimension subject to periodic boundary conditions is given by $L > 0$. Furthermore, the set of translation vectors $\mathcal{S} \subseteq \mathbb{Z}^3$ will be defined later on according to the given boundary conditions. Note that the prime on the double sum indicates that for $\boldsymbol{n} = \boldsymbol{0}$ all terms with $i = j$ are omitted. We are also interested in the forces acting on the particles, which are given by

$$\boldsymbol{F}_{\mathcal{S}}(\boldsymbol{x}_j) := q_j \boldsymbol{E}_{\mathcal{S}}(\boldsymbol{x}_j), \quad \text{with the fields} \quad \boldsymbol{E}_{\mathcal{S}}(\boldsymbol{x}_j) := -\nabla \phi_{\mathcal{S}}(\boldsymbol{x}_j).$$

For the sake of brevity, we will derive fast algorithms for computing the potentials $\phi_{\mathcal{S}}(\boldsymbol{x}_j)$ and skip the analog derivation of algorithms for computing the forces $\boldsymbol{F}_{\mathcal{S}}(\boldsymbol{x}_j)$ within this tutorial.

The different cases of mixed periodic boundary conditions are described as follows. Assume periodic boundary conditions in the first $p \in \{0, 1, 2, 3\}$ dimensions and non-periodic (open) boundary conditions in the remaining $3 - p$ dimensions. Then, we set $\mathcal{S} := \mathbb{Z}^p \times \{0\}^{3-p}$ with $\boldsymbol{x}_j \in [-L/2, L/2)^p \times \mathbb{R}^{3-p}$, i.e., the sum over $\mathcal{S}$ in (1.2) can be interpreted as a replication of the primary box along all dimensions subject to periodic boundary conditions. For a graphical illustration see Figures 1.1 and 1.2.
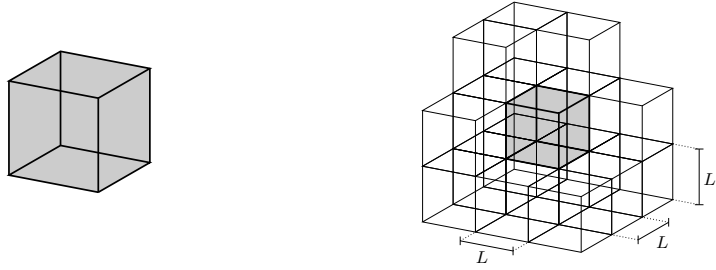

Figure 1.1. In the 0d-periodic case the particles are distributed within a finite box in $\mathbb{R}^3$ (left). In the 3d-periodic case the simulation box with edge length L is duplicated along all three dimensions (right).
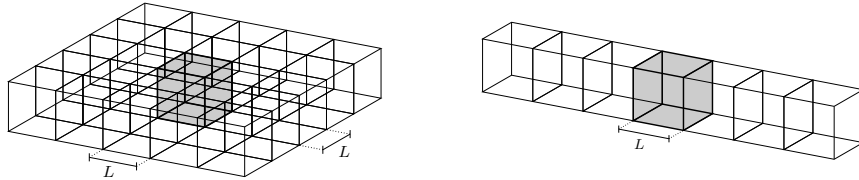

Figure 1.2. The simulation box is duplicated along two of three dimensions in the 2d-periodic case (left) and along one dimension in the 1d-periodic setting (right).

It is important to note that except for open boundary conditions the sum (1.2) is only conditionally convergent, i.e., the values of the potentials $\phi_{\mathcal{S}}(\boldsymbol{x}_j)$ depend on the order of summation. A common definition is to sum up the interactions box wise in a spherically increasing order, i.e.,

$$\phi_{\mathcal{S}}(\boldsymbol{x}_j) := \sum_{t=0}^{\infty} \sum_{\substack{\boldsymbol{n} \in \mathcal{S} \\ \|\boldsymbol{n}\|^2 = t}} \sum_{i=1}^{N}{}' \frac{q_i}{\|\boldsymbol{x}_{ij} + L\boldsymbol{n}\|}. \tag{1.3}$$

The well known Ewald summation technique[16] is the main basis for a variety of fast algorithms for the evaluation of (1.2) under 3d-periodic boundary conditions, see[26, 15, 11, 13, 33].

It is based on the trivial identity

$$\frac{1}{r} = \frac{\mathrm{erfc}(\alpha r)}{r} + \frac{\mathrm{erf}(\alpha r)}{r}. \tag{1.4}$$

Hereby, $\alpha > 0$ is generally known as the splitting parameter, $\mathrm{erf}(x) := \frac{2}{\sqrt{\pi}} \int_0^x \mathrm{e}^{-t^2} \mathrm{d}t$ is the error function and $\mathrm{erfc}(x) := 1 - \mathrm{erf}(x)$ is the complementary error function.

If (1.4) is applied to (1.2), the potential $\phi_{\mathcal{S}}(\boldsymbol{x}_j)$ is split into two parts. Thereby, the sum containing the erfc-terms includes a singularity at $r = 0$ but converges that fast that a good approximation is obtained by only considering few summands. The second part, containing the error function, is still conditionally convergent but exclusively involves smooth and L-periodic functions. The well known Ewald approach transforms this part into a fast convergent Fourier space sum under the implicit assumption of the spherical summation order (1.3). For a derivation in the 3d-periodic case we refer to the paper[12], where convergence factors are applied in order to calculate conditional convergent sum. A similar derivation of the Ewald formulas for the 2d- and 1d-periodic settings can be found in the Appendix of[40].

In the case of 3d-periodic boundary conditions the nonequispaced fast Fourier transform (NFFT)[30] can be directly applied to the Fourier space sum in order to achieve a fast algorithm. For all other kinds of mixed boundary conditions it is also possible to derive fast algorithms based on the NFFT. However, dimensions subject to non-periodic boundary conditions require special treatment in order to get fast convergent Fourier approximations. More precisely, we must embed non-periodic functions into smooth periodic functions, such that their Fourier sum converges rapidly, see Section 2.1 for details.

The outline of this tutorial is as follows. We start with some preliminary remarks about Fourier approximations and give a short introduction to the nonequispaced fast Fourier transform (NFFT) in Section 2. In Section 3 we present the main ideas of the fast Ewald summation for 3d-periodic boundary conditions. In Section 4 we consider the case of periodic boundary conditions in two of three dimensions. Thereby, we follow mainly the presentation from Section 4 in[40]. We continue in Section 5 with the 1d-periodic case in an analog manner as in Section 5 of[40]. Finally we extend the results to 0d-periodic (open) boundary conditions in Section 6. Finally, in Section 7 we conclude the tutorial and give references to numerical results.

2 Prerequisite

In this section we introduce three different concepts from Fouier analysis, which we apply in order to derive the presented algorithms, see Sections 3–6.

2.1 Fourier approximations

In the following, we discuss three different approaches to compute a Fourier approximation of a non-periodic function f within an interval $[-L, L]$.

Variant I (Periodization): The continuous Fourier transform of the function $f \in L^1(\mathbb{R})$ is given by

$$\hat{f}(\xi) = \int_{\mathbb{R}} f(x) \mathrm{e}^{-2\pi \mathrm{i} x \xi} \mathrm{d}x.$$

If f is sufficiently small outside the interval $[-L, L]$, we may approximate f by its h-periodic version $\sum_{n \in \mathbb{Z}} f(\cdot + hn)$, where $h \geq 2L$, apply the Poisson summation formula and truncate the resulting infinite sum in order to obtain an approximation of the form

$$f(x) \approx \sum_{n=-\infty}^{\infty} f(x + hn) = \frac{1}{h} \sum_{l=-\infty}^{\infty} \hat{f}(l/h) e^{2\pi i l r/h}$$

$$\approx \frac{1}{h} \sum_{l=-M/2}^{M/2-1} \hat{f}(l/h) e^{2\pi i l r/h}, \tag{2.1}$$

where $M \in 2\mathbb{N}$ has to be chosen sufficiently large. Alternatively, we could argue as follows. First, we truncate the Fourier integral and, second, we approximate the resulting finite integral via the trapezoidal quadrature rule

$$f(x) = \int_{\mathbb{R}} \hat{f}(\xi) e^{2\pi i x \xi} d\xi \approx \int_{-K/2}^{K/2} \hat{f}(\xi) e^{2\pi i r \xi} d\xi$$

$$\approx \frac{K}{M} \sum_{l=-M/2}^{M/2-1} \hat{f}(\tfrac{lK}{M}) e^{2\pi i r l K/M}. \tag{2.2}$$

Comparison of (2.1) and (2.2) shows that this approach is equivalent to considering a $h = M/K$ periodization of f, as described above.

This approach is limited to functions that decay sufficiently fast in the interval $[-h/2, h/2)$. In other words, whenever f is not sufficiently small we need to choose a relatively large period $h \gg 2L$, which may also result in the choice of a large cutoff M.

Variant II (Truncation): We take a sufficiently large cutoff $h \geq 2L$ and approximate the function f on the interval $[-h/2, h/2]$ by a Fourier series

$$f(x) \approx \sum_{l=M/2}^{M/2-1} c_l e^{2\pi i l x/h},$$

where we compute the coefficients c_l by

$$c_l := \frac{1}{h} \int_{-h/2}^{h/2} f(x) e^{-2\pi i l x/h} dx.$$

Note that the approximated h-periodic function is only smooth of order zero in $r = h/2$, which results in a rather slow second order convergence in Fourier space. Thus, one may have to choose M very large in order to achieve a good approximation. In contrast to Variant I, this approximation approach can be used for non decaying functions f as well.

Variant III (Regularization): Another approach to obtain a Fourier space representation of f is as follows. The key idea is to cutoff f outside the interval $[-L, L]$ but use a Fourier approximation on the slightly larger interval $[-h/2, h/2]$. In the resulting gap $[L, h - L]$ we construct a regularization function that interpolates the derivatives of f at L up to order $p - 1 \in \mathbb{N}$. Therefore, we get a Fourier approximation of a $(p-1)$-times differentiable function which means $(p+1)$-th order convergence in Fourier space. In order to construct the smooth $((p-1)$-times differentiable) transitions we have to regularize the function f. Thereby, we assume that we know the function values and the derivatives in

4

the boundary points (in the following denoted by a_j and b_j) and compute a regularization (in the following denoted by P). The following theorem gives the precise definition of the regularizing function. We remark that in our application we always know the function values and the derivatives in the boundary points. Methods without this knowledge are known as Fourier extensions[28] or Fourier continuations[35].

Theorem 2.1. *Let an interval* $[m - r, m + r], r > 0$, *and the interpolation values* $a_j = f^{(j)}(m - r), b_j = f^{(j)}(m + r), j = 0, \ldots, p - 1$, *be given. For* $y = \frac{x-m}{r}$ *the polynomial*

$$P(x) = \sum_{j=0}^{p-1} B(p, j, y) r^j a_j + \sum_{j=0}^{p-1} B(p, j, -y)(-r)^j b_j,$$

of degree $2p - 1$, *which is defined using the basis polynomials*

$$B(p, j, y) := \sum_{k=0}^{p-1-j} \binom{p-1+k}{k} \frac{1}{j! 2^p 2^k} (1 - y)^p (1 + y)^{k+j},$$

satisfies the interpolation conditions $P^{(j)}(m-r) = a_j, P^{(j)}(m+r) = b_j, j = 0, \ldots, p-1$.

Proof. See Corollary 2.2.6 in[2] or Proposition 3.2 in[17]. $\qquad\square$

In summary, we see some graphical illustrations of the above-mentioned three Fourier approximation variants in Figures 2.1 and 2.2.
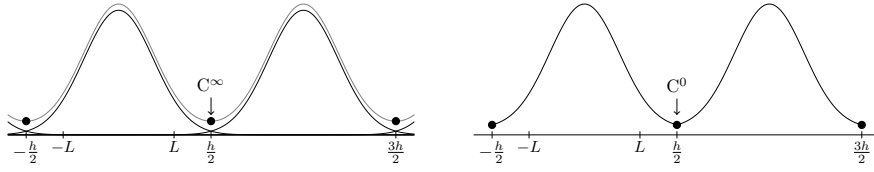
Figure 2.1. Variant I (periodization) on the left and Variant II (truncation) on the right side.
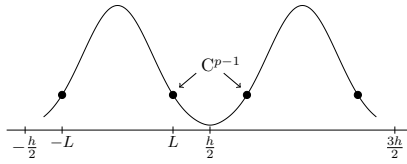
Figure 2.2. Variant III (regularization).

The main advantage of Variant III is that we are able to construct a function of arbitrary smoothness p while the period h can be chosen relatively small compared to the interval length $2L$. On the other hand, the fact that the approximated functions in Variant I are C^∞ makes this approach spectrally accurate. Using Variant II allows us to choose h relatively small. But, the functions are only continuous and of no higher smoothness. Thus, the

Fourier coefficients only decrease rather slow, which also results in the choice of a large cutoff M.

2.2 Nonequispaced discrete Fourier transform (NDFT)

Let the dimension $d \in \mathbb{N}$, the torus $\mathbb{T}^d := \mathbb{R}^d / \mathbb{Z}^d \simeq [-1/2, 1/2)^d$ and the sampling set $\mathcal{X} := \{ \boldsymbol{x}_j \in \mathbb{T}^d \colon j = 1, \ldots, N \}$ with $N \in \mathbb{N}$ be given. Furthermore, let the multi degree $\boldsymbol{M} = (M_1, M_2, \ldots, M_d)^\top \in 2\mathbb{N}^d$ and the index set of possible frequencies

$$\mathcal{I}_{\boldsymbol{M}} := \left\{ -\tfrac{M_1}{2}, \ldots, \tfrac{M_1}{2} - 1 \right\} \times \ldots \times \left\{ -\tfrac{M_d}{2}, \ldots, \tfrac{M_d}{2} - 1 \right\}$$

be given. We define the space of d-variate trigonometric polynomials $T_{\boldsymbol{M}}$ of multi degree $\boldsymbol{M}$ by

$$T_{\boldsymbol{M}} := \operatorname{span} \left\{ \mathrm{e}^{-2\pi \mathrm{i} \boldsymbol{k} \cdot (\cdot)} \colon \boldsymbol{k} \in I_{\boldsymbol{M}} \right\}.$$

The dimension of this space and, hence, the total number of Fourier coefficients is $|\mathcal{I}_{\boldsymbol{M}}| = M_1 \cdot \ldots \cdot M_d$. Note that we abbreviate the inner product between the frequency $\boldsymbol{k}$ and the time/spatial node $\boldsymbol{x}$ by $\boldsymbol{k} \cdot \boldsymbol{x} = k_1 x_1 + k_2 x_2 + \ldots + k_d x_d$. For clarity of presentation the multi index $\boldsymbol{k}$ addresses elements of vectors and matrices as well.

For a finite number $|\mathcal{I}_{\boldsymbol{M}}|$ of given Fourier coefficients $\hat{f}_{\boldsymbol{k}} \in \mathbb{C}$, $\boldsymbol{k} \in \mathcal{I}_{\boldsymbol{M}}$, one wants to evaluate the trigonometric polynomial

$$f(\boldsymbol{x}) := \sum_{\boldsymbol{k} \in \mathcal{I}_{\boldsymbol{M}}} \hat{f}_{\boldsymbol{k}} \mathrm{e}^{-2\pi \mathrm{i} \boldsymbol{k} \cdot \boldsymbol{x}} \in T_{\boldsymbol{M}} \tag{2.3}$$

at given nonequispaced nodes $\boldsymbol{x}_j \in \mathbb{T}^d$, $j = 1, \ldots, N$. Thus, our concern is the computation of the matrix vector product

$$\boldsymbol{f} = \boldsymbol{A}\hat{\boldsymbol{f}}, \tag{2.4}$$

where

$$\boldsymbol{f} := (f(\boldsymbol{x}_j))_{j=1,\ldots,N}, \quad \boldsymbol{A} := \left(\mathrm{e}^{-2\pi \mathrm{i} \boldsymbol{k} \cdot \boldsymbol{x}_j} \right)_{j=1,\ldots,N;\; \boldsymbol{k} \in \mathcal{I}_{\boldsymbol{M}}}, \quad \hat{\boldsymbol{f}} := \left(\hat{f}_{\boldsymbol{k}} \right)_{\boldsymbol{k} \in \mathcal{I}_{\boldsymbol{M}}}.$$

The straightforward algorithm for this matrix vector product, which is called NDFT, takes $\mathcal{O}(N|\mathcal{I}_{\boldsymbol{M}}|)$ arithmetical operations. A related matrix vector product is the adjoint NDFT

$$\hat{\boldsymbol{f}} = \boldsymbol{A}^\mathsf{H} \boldsymbol{f}, \qquad \hat{f}_{\boldsymbol{k}} = \sum_{j=1}^{N} f_j \mathrm{e}^{2\pi \mathrm{i} \boldsymbol{k} \cdot \boldsymbol{x}_j},$$

where $\boldsymbol{A}^\mathsf{H} = \overline{\boldsymbol{A}}^\top$. Furthermore, note that the inversion formula $\boldsymbol{F}^{-1} = \boldsymbol{F}^\mathsf{H}$ for the (equispaced and normalized) Fourier matrix $\boldsymbol{F}$ does **not** hold in the general situation of arbitrary sampling nodes for the matrix $\boldsymbol{A}$.

2.3 Nonequispaced fast Fourier transform (NFFT)

Several algorithms have been proposed for the fast computation of (2.4), cf.[14, 8, 49, 48, 18, 21].
In this section we summarize the main ideas of the most successful approach based
on[48, 32, 30]. It makes use an oversampled FFT and a window function φ that is simultaneously well localized in time/space and frequency domain. Given that the window function
is well localized in spatial domain, its periodic version

$$\tilde{\varphi}(\boldsymbol{x}) := \sum_{\boldsymbol{k} \in \mathbb{Z}^d} \varphi(\boldsymbol{x} + \boldsymbol{k})$$

is well defined.

Throughout the rest of the tutorial we denote by $\sigma \geq 1$ the oversampling factor and by
$m := \sigma M \in \mathbb{N}$ the (oversampled) FFT size (in the case $d = 1$). Furthermore, for $d > 1$
let the vector valued oversampling factor be defined by $\boldsymbol{\sigma} = (\sigma_1, \ldots, \sigma_d)^\top \in \mathbb{R}^d$ (where
$\sigma_1, \ldots, \sigma_d \geq 1$) and the FFT size be denoted by $\boldsymbol{m} := \boldsymbol{\sigma} \odot \boldsymbol{M}$. For notational convenience
we use the pointwise product

$$\boldsymbol{\sigma} \odot \boldsymbol{M} := (\sigma_1 M_1, \sigma_2 M_2, \ldots, \sigma_d M_d,)^\top$$

and the point wise inverse

$$\boldsymbol{M}^{-1} := \left(M_1^{-1}, M_2^{-1}, \ldots, M_d^{-1} \right)^\top .$$

The main idea is now to approximate the function f by a sum of translates of the one-periodic function $\tilde{\varphi}$, i.e.,

$$f(\boldsymbol{x}) \approx \sum_{\boldsymbol{l} \in \mathcal{I}_{\boldsymbol{m}}} g_l \tilde{\varphi}(\boldsymbol{x} - \boldsymbol{l} \odot \boldsymbol{m}^{-1}),$$

where we use $\boldsymbol{m} \geq \boldsymbol{M}$ sampling points/translates.

A transformation into Fourier space gives

$$f(\boldsymbol{x}) \approx \sum_{\boldsymbol{k} \in \mathcal{I}_{\boldsymbol{m}}} \sum_{\boldsymbol{r} \in \mathbb{Z}^d} \hat{g}_{\boldsymbol{k}} c_{\boldsymbol{k}}(\tilde{\varphi}) \mathrm{e}^{-2\pi \mathrm{i}(\boldsymbol{k} + \boldsymbol{r} \odot \boldsymbol{m}) \cdot \boldsymbol{x}} \tag{2.5}$$

with the help of the well known convolution theorem. A comparison of (2.3) and (2.5)
shows that it is reasonable to set

$$\hat{g}_{\boldsymbol{k}} := \begin{cases} \frac{\hat{f}_{\boldsymbol{k}}}{c_{\boldsymbol{k}}(\tilde{\varphi})} & : \boldsymbol{k} \in \mathcal{I}_{\boldsymbol{M}}, \\ 0 & : \text{else.} \end{cases} \tag{2.6}$$

The final algorithm can basically be divided into three steps (building blocks) and can
be summarized as follows.

1. Deconvolve the trigonometric polynomial $f \in T_{\boldsymbol{M}}$ in (2.3) with a window function
   in frequency domain, see (2.6).

2. Compute an FFT on the result of step 1.:

$$g_l := \frac{1}{|\mathcal{I}_{\boldsymbol{m}}|} \sum_{\boldsymbol{k} \in \mathcal{I}_{\boldsymbol{m}}} \hat{g}_{\boldsymbol{k}} \mathrm{e}^{-2\pi \mathrm{i} \boldsymbol{k} \cdot (\boldsymbol{l} \odot \boldsymbol{m}^{-1})}, \quad \boldsymbol{l} \in \mathcal{I}_{\boldsymbol{m}}.$$

3. Convolve the result of step 2. with the window function in time/spatial domain, i.e., evaluate this convolution at the nodes $\boldsymbol{x}_j$, $j = 1, \ldots, N$:

$$f(\boldsymbol{x}_j) \approx \sum_{\boldsymbol{l} \in \mathcal{I}_m} g_{\boldsymbol{l}} \tilde{\varphi}(\boldsymbol{x}_j - \boldsymbol{l} \odot \boldsymbol{m}^{-1}).$$

Obviously, we end up with a complexity of $\mathcal{O}(|\mathcal{I}_M| \log |\mathcal{I}_M| + N)$ arithmetic operations. Thereby, the prefactors depend on the required accuracy as well as the properties of the window function. For a description of the NFFT in its matrix-vector notation we refer to[48]. Note that the adjoint NDFT can be approximated in a very similar way by an adjoint NFFT and yields the same enhanced arithmetic complexity. Error bounds in the ∞–norm have already been derived for a variety of possible window functions, see[49,47] for instance. For error estimates in the L_2-norm as well as an automated tuned NFFT see[39]. A widely used implementation is available as part of the NFFT package[29] and is based on the FFTW[20]. This package also offers support of shared memory parallelism[50]. A parallel implementation for graphic processing units was proposed in[31]. Furthermore, an MPI-based parallel NFFT (PNFFT) implementation with support for distributed memory parallelism was proposed in[45] and is publicly available[42]. It is based on a highly scalable MPI extension of FFTW called PFFT[43,41].

3 Fast Ewald summation for 3d–periodic boundary conditions

For an electrical neutral system (1.1) of N charges q_j distributed in a cubic box of edge length L we define the electrostatic potential subject to 3d–periodic boundary conditions by

$$\phi^{\mathrm{p3}}(\boldsymbol{x}_j) := \phi_{\mathbb{Z}^3}(\boldsymbol{x}_j) = \sum_{s=0}^{\infty} \sum_{\substack{\boldsymbol{n} \in \mathbb{Z}^3 \\ \|\boldsymbol{n}\|^2 = s}} \sum_{i=1}^{N}{}' \frac{q_i}{\|\boldsymbol{x}_{ij} + L\boldsymbol{n}\|},$$

i.e., we set $\mathcal{S} := \mathbb{Z}^3$ within the definition (1.3). Remember that the order of summation has to be specified because of the conditional convergence of the infinite sum, as already pointed out in the introduction.

The following formula was at first presented in[16] by using the Ewald splitting. For a derivation based on convergence factors, see[12]. We have

$$\phi^{\mathrm{p3}}(\boldsymbol{x}_j) = \phi^{\mathrm{p3,S}}(\boldsymbol{x}_j) + \phi^{\mathrm{p3,L}}(\boldsymbol{x}_j) + \phi^{\mathrm{p3,self}}(\boldsymbol{x}_j), \tag{3.1}$$

where for the splitting parameter $\alpha > 0$ we define the short range part

$$\phi^{\mathrm{p3,S}}(\boldsymbol{x}_j) := \sum_{\boldsymbol{n} \in \mathbb{Z}^3} \sum_{i=1}^{N}{}' q_i \frac{\mathrm{erfc}(\alpha\|\boldsymbol{x}_{ij} + L\boldsymbol{n}\|)}{\|\boldsymbol{x}_{ij} + L\boldsymbol{n}\|},$$

the long range part

$$\phi^{\mathrm{p3,L}}(\boldsymbol{x}_j) := \frac{1}{\pi L} \sum_{\boldsymbol{k} \in \mathbb{Z}^3 \setminus \{\boldsymbol{0}\}} \frac{\mathrm{e}^{-\pi^2\|\boldsymbol{k}\|^2/(\alpha^2 L^2)}}{\|\boldsymbol{k}\|^2} \left(\sum_{i=1}^{N} q_i \mathrm{e}^{2\pi\mathrm{i}\boldsymbol{k}\cdot\boldsymbol{x}_i/L} \right) \mathrm{e}^{-2\pi\mathrm{i}\boldsymbol{k}\cdot\boldsymbol{x}_j/L},$$

8

and the self potential

$$\phi^{\mathrm{p3,self}}(\boldsymbol{x}_j) := -\frac{2\alpha}{\sqrt{\pi}} q_j.$$

Often a fourth term, the so called dipole correction, appears in the decomposition (3.1), cf.[13]. The dipole correction term is the only part depending on the order of summation. However, if a spherical summation order is applied, the dipole correction term depends only on the norm of the dipole moment $\sum_{j=1}^{N} q_j \boldsymbol{x}_j$ and, additionally, on the dielectric constant of the surrounding medium. Therefore, it can be computed efficiently in $\mathcal{O}(N)$ arithmetic operations. If the medium is assumed to be metallic, the dipole term vanishes and (3.1) applies. It should be mentioned that the formulas above can be generalized to non-cubic boxes and also non-orthogonal (triclinic) boxes, cf.[16,11,27].

Since the complementary error function erfc rapidly tends to zero, the short range part of each potential $\phi^{\mathrm{p3,S}}(\boldsymbol{x}_j)$ can be obtained by direct evaluation, i.e., all distances $\|\boldsymbol{x}_{ij} + L\boldsymbol{n}\|$ larger than an appropriate cutoff radius $r_{\mathrm{cut}} > 0$ are ignored. If we assume a sufficiently homogenous particle distribution, each particle only interacts with a fixed number of neighbors. Thus, the real space sum can be computed with a linked cell algorithm[19] in $\mathcal{O}(N)$ arithmetic operations for this case.

In order to compute the long range parts $\phi^{\mathrm{p3,L}}(\boldsymbol{x}_j)$ we truncate the infinite sum and compute approximations of the sums

$$\hat{S}(\boldsymbol{k}) := \sum_{i=1}^{N} q_i \mathrm{e}^{2\pi\mathrm{i}\boldsymbol{k}\cdot\boldsymbol{x}_i/L}, \quad \boldsymbol{k} \in \mathcal{I}_{\boldsymbol{M}},$$

with an adjoint NFFT and evaluate

$$\phi^{\mathrm{p3,L}}(\boldsymbol{x}_j) \approx \sum_{\boldsymbol{k} \in \mathcal{I}_{\boldsymbol{M}}\setminus\{\boldsymbol{0}\}} \hat{b}_{\boldsymbol{k}} \hat{S}(\boldsymbol{k}) \mathrm{e}^{-2\pi\mathrm{i}\boldsymbol{k}\cdot\boldsymbol{x}_j/L}, \quad j = 1, \ldots, N,$$

via the NFFT. Thereby, we define the Fourier coefficients

$$\hat{b}_{\boldsymbol{k}} := \frac{1}{\pi L} \frac{\mathrm{e}^{-\pi^2\|\boldsymbol{k}\|^2/(\alpha^2 L^2)}}{\|\boldsymbol{k}\|^2}.$$

The proposed evaluation of $\phi^{\mathrm{p3,L}}(\boldsymbol{x}_j)$ at the points $\boldsymbol{x}_j$, $j = 1, \ldots, N$, requires $\mathcal{O}(N + |\mathcal{I}_{\boldsymbol{M}}| \log |\mathcal{I}_{\boldsymbol{M}}|)$ arithmetic operations.

In matrix vector notation we may write

$$\left(\phi^{\mathrm{p3,L}}(\boldsymbol{x}_j)\right)_{j=1}^{N} \approx \tilde{\boldsymbol{A}} \boldsymbol{D} \tilde{\boldsymbol{A}}^{\mathsf{H}} \boldsymbol{q}, \tag{3.2}$$

where $\tilde{\boldsymbol{A}} \approx \boldsymbol{A}$ denotes the matrix representation of the NFFT ($\approx$NDFT) in three dimensions, $\boldsymbol{D}$ is a diagonal matrix with entries $\hat{b}_{\boldsymbol{k}}$, $\boldsymbol{k} \in \mathcal{I}_{\boldsymbol{M}}$, and $\boldsymbol{q} = (q_1, \ldots, q_N)^{\top} \in \mathbb{R}^N$.

Relations to existing work

A straightforward method, that accelerates the traditional Ewald summation technique by NFFT was already presented in[44]. This combination was first presented in[25] is very similar to the FFT-accelerated Ewald sum methods, namely, the so-called particle-particle particle-mesh ($\mathrm{P}^3\mathrm{M}$), particle-mesh Ewald (PME) and smooth particle-mesh Ewald (SPME), see[13] and also[51].

4 Fast Ewald summation for 2d-periodic boundary conditions

In this section we denote for $\boldsymbol{y} = (y_1, y_2, y_3) \in \mathbb{R}^3$ the vector of its first two components by $\tilde{\boldsymbol{y}} := (y_1, y_2) \in \mathbb{R}^2$, $j = 1, \ldots, N$. We consider an electrical neutral system (1.1) of N charges $q_j \in \mathbb{R}$ at positions $\boldsymbol{x}_j = (\tilde{\boldsymbol{x}}_j, x_{j,3}) \in L\mathbb{T}^2 \times \mathbb{R}$. Under periodic boundary conditions in the first two dimensions we define the potential of each single particle by

$$\phi^{\mathrm{p}2}(\boldsymbol{x}_j) := \phi_{\mathbb{Z}^2 \times \{0\}}(\boldsymbol{x}_j) = \sum_{s=0}^{\infty} \sum_{\substack{\boldsymbol{n} \in \mathbb{Z}^2 \times \{0\} \\ \|\boldsymbol{n}\|^2 = s}} \sum_{i=1}^{N}{}' \frac{q_i}{\|\boldsymbol{x}_{ij} + L\boldsymbol{n}\|},$$

i.e., we set $\mathcal{S} := \mathbb{Z}^2 \times \{0\}$ within the definition (1.3). This can be rewritten in the form

$$\phi^{\mathrm{p}2}(\boldsymbol{x}_j) = \phi^{\mathrm{p}2,\mathrm{S}}(\boldsymbol{x}_j) + \phi^{\mathrm{p}2,\mathrm{L}}(\boldsymbol{x}_j) + \phi^{\mathrm{p}2,\boldsymbol{0}}(\boldsymbol{x}_j) + \phi^{\mathrm{p}2,\mathrm{self}}(\boldsymbol{x}_j), \tag{4.1}$$

where for some $\alpha > 0$ we define the short range part

$$\phi^{\mathrm{p}2,\mathrm{S}}(\boldsymbol{x}_j) := \sum_{\boldsymbol{n} \in \mathbb{Z}^2 \times \{0\}} \sum_{i=1}^{N}{}' q_i \frac{\mathrm{erfc}(\alpha \|\boldsymbol{x}_{ij} + L\boldsymbol{n}\|)}{\|\boldsymbol{x}_{ij} + L\boldsymbol{n}\|},$$

the long range parts

$$\phi^{\mathrm{p}2,\mathrm{L}}(\boldsymbol{x}_j) := \frac{1}{2L} \sum_{\boldsymbol{k} \in \mathbb{Z}^2 \setminus \{\boldsymbol{0}\}} \sum_{i=1}^{N} q_i \, \mathrm{e}^{2\pi \mathrm{i} \boldsymbol{k} \cdot \tilde{\boldsymbol{x}}_{ij}/L} \cdot \Theta^{\mathrm{p}2}(\|\boldsymbol{k}\|, x_{ij,3}),$$

$$\phi^{\mathrm{p}2,\boldsymbol{0}}(\boldsymbol{x}_j) := -\frac{2\sqrt{\pi}}{L^2} \sum_{i=1}^{N} q_i \Theta_0^{\mathrm{p}2}(x_{ij,3}), \tag{4.2}$$

the self potential

$$\phi^{\mathrm{p}2,\mathrm{self}}(\boldsymbol{x}_j) := -\frac{2\alpha}{\sqrt{\pi}} q_j \,,$$

and the functions $\Theta^{\mathrm{p}2}(k, r)$, $\Theta_0^{\mathrm{p}2}(r)$ for $k, r \in \mathbb{R}$ are defined by

$$\Theta^{\mathrm{p}2}(k, r) := \frac{1}{k} \left[\mathrm{e}^{2\pi k r/L} \, \mathrm{erfc}\left(\frac{\pi k}{\alpha L} + \alpha r \right) + \mathrm{e}^{-2\pi k r/L} \, \mathrm{erfc}\left(\frac{\pi k}{\alpha L} - \alpha r \right) \right],$$

$$\Theta_0^{\mathrm{p}2}(r) := \frac{\mathrm{e}^{-\alpha^2 r^2}}{\alpha} + \sqrt{\pi} r \, \mathrm{erf}(\alpha r).$$

These expressions were already given in[23]. In the Appendix of[40] we give a proof using convergence factors, similar to the proof of the 3d-periodic case in[12]. Thereby, we always start with the splitting (1.4) and then use the technique of convergence factors to derive the Fourier space representation of the long range part by applying the Poisson summation formula.

The evaluation of the short range part $\phi^{\mathrm{p}2,\mathrm{S}}(\boldsymbol{x}_j)$ is again done by a direct evaluation. For the computation of the long range part we truncate the infinite sum in $\phi^{\mathrm{p}2,\mathrm{L}}(\boldsymbol{x}_j)$, i.e., for some appropriate $\tilde{\boldsymbol{M}} = (M_1, M_2) \in 2\mathbb{N}^2$ we set

$$\phi^{\mathrm{p}2,\mathrm{L}}(\boldsymbol{x}_j) \approx \frac{1}{2L} \sum_{\boldsymbol{k} \in \mathcal{I}_{\tilde{M}} \setminus \{\boldsymbol{0}\}} \sum_{i=1}^{N} q_i \mathrm{e}^{2\pi \mathrm{i} \boldsymbol{k} \cdot \tilde{\boldsymbol{x}}_{ij}/L} \Theta^{\mathrm{p}2}(\|\boldsymbol{k}\|, x_{ij,3}).$$

and apply the regularization Variant III from Section 2.1 to the functions $\Theta^{p2}(\|\boldsymbol{k}\|, \cdot)$. To this end we assume without loss of generality $L_3 > 0$ large enough such that $x_{j,3} \in [-L_3/2, L_3/2]$, i.e., the particle coordinates are bounded also in the non-periodic dimension. Thus, all the functions $\Theta^{p2}(\|\boldsymbol{k}\|, \cdot)$ have to be evaluated only within the finite interval $[-L_3, L_3]$. Note that we have to double the interval length since we do not have periodicity in the last dimension. The same approximation idea is applied to the kernel function $\Theta_0^{p2}(r)$ in (4.2). Note that $\lim_{x\to\pm\infty}[\mathrm{e}^{-x^2} + \sqrt{\pi}x\ \mathrm{erf}(x)] = \lim_{x\to\pm\infty}|x| = \infty$, i.e., the approximation Variant I given in Section 2.1 is not applicable.

At first, we choose $h > 2L_3$ and accordingly some $\varepsilon \in (0, 1/2)$ such that $|x_{ij,3}| \leq L_3 =: h(1/2 - \varepsilon) < h/2$ for all $i, j = 1, \ldots, N$. This corresponds to a surrounding box that is large enough to hold all differences of particle coordinates in the last dimension. In addition, since the strong inequality $h > 2L_3$ holds we have some extra space for constructing a regularization. In order to approximate the long range parts $\phi^{p2,\mathrm{L}}(\boldsymbol{x}_j) + \phi^{p2,\mathbf{0}}(\boldsymbol{x}_j)$ efficiently we consider for $k \in \{\|\boldsymbol{k}\| : \boldsymbol{k} \in \mathcal{I}_{\tilde{\boldsymbol{M}}}\}$ the regularizations

$$K_{\mathrm{R}}(k, r) := \begin{cases} \dfrac{1}{2L}\Theta^{p2}(k, r) & : k \neq 0, |h^{-1}r| \leq 1/2 - \varepsilon, \\ -\dfrac{2\sqrt{\pi}}{L^2}\Theta_0^{p2}(r) & : k = 0, |h^{-1}r| \leq 1/2 - \varepsilon, \\ K_{\mathrm{B}}(k, r) & : |h^{-1}r| \in (1/2 - \varepsilon, 1/2], \end{cases} \tag{4.3}$$

where we claim that each function $K_{\mathrm{B}}(k, \cdot) : [-h/2, -h/2 + h\varepsilon] \cup [h/2 - h\varepsilon, h/2] \to \mathbb{R}$ fulfills the Hermite interpolation conditions

$$\frac{\partial^j}{\partial r^j}K_{\mathrm{B}}(k, h/2 - h\varepsilon) = \begin{cases} \frac{1}{2L}\frac{\partial^j}{\partial r^j}\Theta^{p2}(k, h/2 - h\varepsilon) & : k \neq 0, \\ -\frac{2\sqrt{\pi}}{L^2}\frac{\mathrm{d}^j}{\mathrm{d}r^j}\Theta_0^{p2}(h/2 - h\varepsilon) & : k = 0, \end{cases} \tag{4.4}$$

$$\frac{\partial^j}{\partial r^j}K_{\mathrm{B}}(k, -h/2 + h\varepsilon) = \begin{cases} \frac{1}{2L}\frac{\partial^j}{\partial r^j}\Theta^{p2}(k, -h/2 + h\varepsilon) & : k \neq 0, \\ -\frac{2\sqrt{\pi}}{L^2}\frac{\mathrm{d}^j}{\mathrm{d}r^j}\Theta_0^{p2}(-h/2 + h\varepsilon) & : k = 0, \end{cases} \tag{4.5}$$

for all $j = 0, \ldots, p - 1$. Hereby, we refer to $p \in \mathbb{N}$ as the degree of smoothness. In order to end up with h-periodic, smooth functions $K_{\mathrm{R}}(k, \cdot)$, the functions $K_{\mathrm{B}}(k, \cdot)$ are constructed such that

$$\frac{\partial^j}{\partial r^j}K_{\mathrm{R}}(k, h/2) = \frac{\partial^j}{\partial r^j}K_{\mathrm{R}}(k, -h/2) \quad \text{for } j = 0, \ldots, p - 1$$

is also fulfilled. In Theorem 2.1 we show that the functions $K_{\mathrm{B}}(k, .)$ can be constructed as polynomials of degree $2p - 1$ by two point Taylor interpolation. Figure 4.1 shows an example of such a regularization $K_{\mathrm{R}}(k, \cdot)$.

In summary, the functions $K_{\mathrm{R}}(k, \cdot)$ are h-periodic and smooth, i.e., $K_{\mathrm{R}}(k, \cdot) \in C^{p-1}(h\mathbb{T})$. Therefore, they can be approximated by a truncated Fourier series up to a prescribed error. To this end, we approximate for each $k \in \{\|\boldsymbol{k}\| \neq 0 : \boldsymbol{k} \in \mathcal{I}_{\tilde{\boldsymbol{M}}}\}$ the function

$$\frac{1}{2L}\Theta^{p2}(k, r) \approx \sum_{l\in\mathcal{I}_{M_3}} \hat{b}_{k,l}\mathrm{e}^{2\pi\mathrm{i}lr/h} \tag{4.6}$$

for $|r| \leq h/2 - h\varepsilon = L_3$ by the truncated Fourier series of its regularization $K_{\mathrm{R}}(k, \cdot)$.
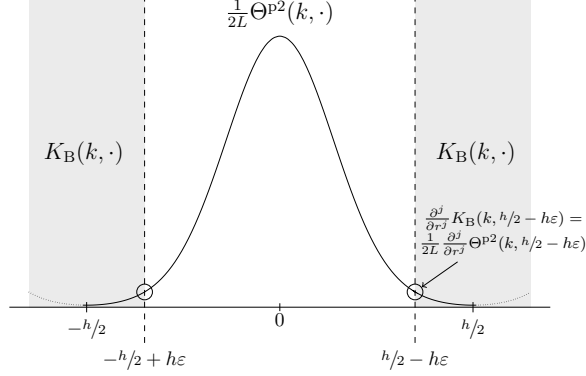
Figure 4.1. Example for $K_R(k, \cdot)$ for $k \geq 1$. At the boundaries (gray area) the regularization adopts the values of the boundary function $K_B(k, \cdot)$. We also marked the points, where the conditions (4.4) and (4.5) are fulfilled. In our implementation, the function in the gray area is a polynomial of degree $2p - 1$ constructed by two-point Taylor interpolation.

Analogously, for $k = 0$ we have

$$-\frac{2\sqrt{\pi}}{L^2} \Theta_0^{p2}(r) \approx \sum_{l \in \mathcal{I}_{M_3}} \hat{b}_{0,l} e^{2\pi i l r/h}. \tag{4.7}$$

Thereby, we choose the frequency cutoff $M_3 \in 2\mathbb{N}$ large enough and compute the Fourier coefficients $\hat{b}_{k,l}$ in (4.6) as well as $\hat{b}_{0,l}$ in (4.7) by the discrete Fourier transform

$$\hat{b}_{k,l} := \frac{1}{M_3} \sum_{j \in \mathcal{I}_{M_3}} K_R\left(k, \frac{jh}{M_3}\right) e^{-2\pi i j l/M_3}, \qquad l = -M_3/2, \dots, M_3/2 - 1.$$

This ansatz is closely related to the fast summation method described in[47]. Due to the fact that we have $\Theta_0^{p2}(\cdot), \Theta^{p2}(k, \cdot) \in C^\infty(\mathbb{R})$ ($k \geq 1$) we are not restricted in the choice of the parameter p. By choosing M_3 large enough we can construct approximations (4.6) and (4.7) of a required accuracy.

If $k \in \{\|\boldsymbol{k}\| \neq 0 : \boldsymbol{k} \in \mathcal{I}_{\tilde{\boldsymbol{M}}}\}$ is large enough, then the function value $\Theta^{p2}(k, h/2)$ might be sufficiently small so that

$$\Theta^{p2}(k, r) \approx \sum_{n \in \mathbb{Z}} \Theta^{p2}(k, r + hn),$$

yields a good approximation, see Figure 4.2.

In this case we could also apply Variant I, as described in Section 2. The analytical Fourier transform of $\Theta^{p2}(k, \cdot)$ is given by

$$\hat{\Theta}^{p2}(k, \xi) = \int_{-\infty}^{\infty} \Theta^{p2}(k, r) e^{-2\pi i r \xi} dr = \frac{2L}{\pi(k^2 + L^2 \xi^2)} e^{-\pi^2 k^2/(\alpha^2 L^2) - \pi^2 \xi^2/\alpha^2},$$

see[34], for instance. Applying the Poisson summation formula leads to

$$\frac{1}{2L} \Theta^{p2}(k, r) \approx \frac{1}{2L} \sum_{n \in \mathbb{Z}} \Theta^{p2}(k, r + hn) \approx \frac{1}{2Lh} \sum_{l \in \mathcal{I}_{M_3}} \hat{\Theta}^{p2}(k, l/h) e^{2\pi i l r/h},$$
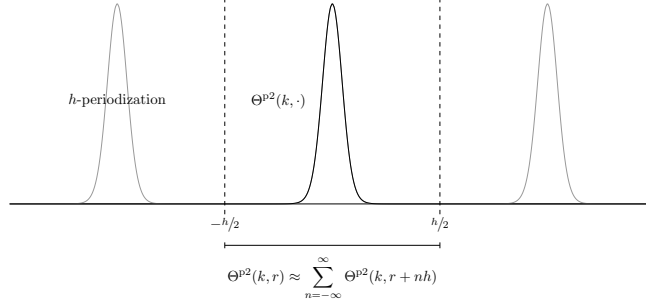
Figure 4.2. If k is sufficiently large, the h-periodic version of $\Theta^{\mathrm{p}2}(k,\cdot)$ might be a good approximation of $\Theta^{\mathrm{p}2}(k,\cdot)$.

i.e., we can simply set $\hat{b}_{k,l} := (2Lh)^{-1}\hat{\Theta}^{\mathrm{p}2}(k,{}^l/_h)$ instead of regularizing the function.

In summary, we obtain the following approximation for the long range parts,

$$\phi^{\mathrm{p}2,\mathrm{L}}(\boldsymbol{x}_j) + \phi^{\mathrm{p}2,\mathbf{0}}(\boldsymbol{x}_j) \approx \sum_{\boldsymbol{k}\in\mathcal{I}_{\tilde{M}}} \sum_{l\in\mathcal{I}_{M_3}} \hat{b}_{\|\boldsymbol{k}\|,l} \sum_{i=1}^{N} q_i \mathrm{e}^{2\pi\mathrm{i}\boldsymbol{k}\cdot\tilde{\boldsymbol{x}}_{ij}/L} \mathrm{e}^{2\pi\mathrm{i}l x_{ij,3}/h}$$

$$= \sum_{(\boldsymbol{k},l)\in\mathcal{I}_{\boldsymbol{M}}} \hat{b}_{\|\boldsymbol{k}\|,l} \left(\sum_{i=1}^{N} q_i \mathrm{e}^{2\pi\mathrm{i}\boldsymbol{v}(\boldsymbol{k},l)\cdot\boldsymbol{x}_i} \right) \mathrm{e}^{-2\pi\mathrm{i}\boldsymbol{v}(\boldsymbol{k},l)\cdot\boldsymbol{x}_j},$$

where we substitute the truncated Fourier series (4.6), (4.7) into (4.1), (4.2) and define $\boldsymbol{M} := (\tilde{\boldsymbol{M}}, M_3) \in 2\mathbb{N}^3$ as well as the vectors $\boldsymbol{v}(\boldsymbol{k},l) := (\boldsymbol{k}/L, l/h) \in L^{-1}\mathbb{Z}^2 \times h^{-1}\mathbb{Z}$. The expressions in the inner brackets

$$\hat{S}(\boldsymbol{k},l) := \sum_{i=1}^{N} q_i \mathrm{e}^{2\pi\mathrm{i}\boldsymbol{v}(\boldsymbol{k},l)\cdot\boldsymbol{x}_i}, \quad (\boldsymbol{k},l) \in \mathcal{I}_{\boldsymbol{M}},$$

can be computed by an adjoint NFFT. This will be followed by $|\mathcal{I}_{\boldsymbol{M}}|$ multiplications with $\hat{b}_{\|\boldsymbol{k}\|,l}$ and completed by an NFFT to compute the outer summation over the indexes $(\boldsymbol{k},l) \in \mathcal{I}_{\boldsymbol{M}}$. Therefore, the proposed evaluation of $\phi^{\mathrm{p}2,\mathrm{L}}(\boldsymbol{x}_j) + \phi^{\mathrm{p}2,\mathbf{0}}(\boldsymbol{x}_j)$ at the points $\boldsymbol{x}_j, j = 1,\ldots,N$, requires $\mathcal{O}(N + |\mathcal{I}_{\boldsymbol{M}}|\log|\mathcal{I}_{\boldsymbol{M}}|)$ arithmetic operations.

We obtain a similar matrix-vector notation as in the 3d-periodic case, namely,

$$\left(\phi^{\mathrm{p}2,\mathrm{L}}(\boldsymbol{x}_j) + \phi^{\mathrm{p}2,\mathbf{0}}(\boldsymbol{x}_j)\right)_{j=1}^{N} \approx \tilde{\boldsymbol{A}}\boldsymbol{D}\tilde{\boldsymbol{A}}^{\mathsf{H}}\boldsymbol{q}, \tag{4.8}$$

where $\tilde{\boldsymbol{A}}$ denotes the matrix representation of the NFFT in three dimensions for the nodes $(\tilde{\boldsymbol{x}}_j/L, x_{j,3}/h) \in \mathbb{T}^3$, $\boldsymbol{D}$ is a diagonal matrix with entries $\hat{b}_{\|\boldsymbol{k}\|,l}$, $(\boldsymbol{k},l) \in \mathcal{I}_{\boldsymbol{M}}$, and $\boldsymbol{q} = (q_1,\ldots,q_N)^{\top} \in \mathbb{R}^N$.

Relations to existing work

The Ewald formulas (4.1) for 2d-periodic geometries were already proposed in[23]. We remark that a method based on the splitting (4.1) is used in[34] in combination with Variant I of

Section 2. As pointed out on page 12 in[34] this approach is limited to functions that decay sufficiently fast in the interval $[-h/2, h/2)$. In other words, whenever $\Theta^{\mathrm{p}2}(k, \max|x_{ij,3}|)$ is not sufficiently small we need to choose a relatively large period $h \gg 2L$, which may also result in the choice of a large cutoff M_3. Some other Fourier based algorithms, like MMM2D[6] or ELC[3] already exist. A method based on approximation Variant II from Section 2.1 is proposed in[38]. However, as mentioned in Section 2.1 this method suffers from the rather slow convergence rate in Fourier space. See also[52,9] for algorithms with higher complexity.

5   Fast Ewald summation for 1d-periodic boundary conditions

In this section we denote for some $\boldsymbol{y} = (y_1, y_2, y_3) \in \mathbb{R}^3$ the vector of its last two components by $\tilde{\boldsymbol{y}} := (y_2, y_3) \in \mathbb{R}^2$. We consider a system of N charges $q_j \in \mathbb{R}$ at positions $\boldsymbol{x}_j = (x_{j,1}, \tilde{\boldsymbol{x}}_j) \in L\mathbb{T} \times \mathbb{R}^2$, $j = 1, \ldots, N$. If periodic boundary conditions are assumed only in the first coordinate we define the potential of each single particle j by

$$\phi^{\mathrm{p}1}(\boldsymbol{x}_j) := \phi_{\mathbb{Z} \times \{0\}^2}(\boldsymbol{x}_j) = \sum_{s=0}^{\infty} \sum_{\substack{\boldsymbol{n} \in \mathbb{Z} \times \{0\}^2 \\ |n_1| = s}} \sum_{i=1}^{N} {}' \frac{q_i}{\|\boldsymbol{x}_{ij} + L\boldsymbol{n}\|} \tag{5.1}$$

i.e., we set $\mathcal{S} := \mathbb{Z} \times \{0\}^2$ within definition (1.3). In the following we denote by

$$\Gamma(s, x) := \int_x^{\infty} t^{s-1} \mathrm{e}^{-t} \mathrm{d}t$$

the upper incomplete gamma function. For the case $s = 0$ the well known identity

$$\Gamma(0, x) = -\gamma - \ln x - \sum_{k=1}^{\infty} (-1)^k \frac{x^k}{k!k}$$

holds for all positive x, see [number 5.1.11] in[1]. Thereby, γ is the Euler-Mascheroni constant. The function $\Gamma(0, \cdot)$ is also known as the exponential integral function. We easily see

$$\lim_{x \to 0} \Gamma(0, x) + \ln x + \gamma = 0.$$

The potential (5.1) can be written as

$$\phi^{\mathrm{p}1}(\boldsymbol{x}_j) = \phi^{\mathrm{p}1,\mathrm{S}}(\boldsymbol{x}_j) + \phi^{\mathrm{p}1,\mathrm{L}}(\boldsymbol{x}_j) + \phi^{\mathrm{p}1,0}(\boldsymbol{x}_j) + \phi^{\mathrm{p}1,\mathrm{self}}(\boldsymbol{x}_j),$$

where for the splitting parameter $\alpha > 0$ we define the short range part

$$\phi^{\mathrm{p}1,\mathrm{S}}(\boldsymbol{x}_j) := \sum_{\boldsymbol{n} \in \mathbb{Z} \times \{0\}^2} \sum_{i=1}^{N} {}' q_i \frac{\mathrm{erfc}(\alpha\|\boldsymbol{x}_{ij} + L\boldsymbol{n}\|)}{\|\boldsymbol{x}_{ij} + L\boldsymbol{n}\|},$$

the long range parts

$$\phi^{\mathrm{p1,L}}(\boldsymbol{x}_j) := \frac{2}{L} \sum_{k \in \mathbb{Z} \backslash \{0\}} \sum_{i=1}^{N} q_i \, \mathrm{e}^{2\pi \mathrm{i}k(x_{i,1}-x_{j,1})/L} \cdot \Theta^{\mathrm{p1}}(k, \|\tilde{\boldsymbol{x}}_{ij}\|)\,, \qquad (5.2)$$

$$\phi^{\mathrm{p1,0}}(\boldsymbol{x}_j) := -\frac{1}{L} \sum_{\substack{i=1 \\ \|\tilde{\boldsymbol{x}}_{ij}\| \neq 0}}^{N} q_i \Theta_0^{\mathrm{p1}}(\|\tilde{\boldsymbol{x}}_{ij}\|)\,, \qquad (5.3)$$

the self potential

$$\phi^{\mathrm{p1,self}}(\boldsymbol{x}_j) := -\frac{2\alpha}{\sqrt{\pi}}q_j \,,$$

and the functions $\Theta^{\mathrm{p1}}(k,r), \Theta_0^{\mathrm{p1}}(r)$ for $k, r \in \mathbb{R}$ are defined by

$$\Theta^{\mathrm{p1}}(k,r) := \int_0^\alpha \frac{1}{z}\mathrm{e}^{\frac{-\pi^2 k^2}{L^2 z^2}}\mathrm{e}^{-r^2 z^2}\mathrm{d}z,$$

$$\Theta_0^{\mathrm{p1}}(k,r) := \gamma + \Gamma(0, \alpha^2 r^2) + \ln(\alpha^2 r^2)\,.$$

The function $\Theta^{\mathrm{p1}}(k,r)$ can be expressed by the incomplete modified Bessel function of the second kind[24], see Section 5.2.2 in[40]. This function is known to be indefinitely often differentiable and, thus, we can construct regularizations of similar structure as (4.3) in order to construct a fast algorithm. In this case the final algorithm requires a smooth bivariate regularization, which can be obtained easily from a one dimensional construction as the Fourier coefficients are radial in $\tilde{\boldsymbol{x}}_{ij}$.

By the Lemma 5.2 in[40] we show that the function $\Theta^{\mathrm{p1}}(k,r)$ for fixed r tends to zero exponentially fast for growing k, which allows the truncation of the infinite sum in $\phi^{\mathrm{p1,L}}(\boldsymbol{x}_j)$. Furthermore, Lemma 5.3 in[40] shows that also the kernel in $\phi^{\mathrm{p1,0}}(\boldsymbol{x}_j)$ is a smooth function, which allows the application of the fast summation method. Note that we have $\lim_{x \to \pm\infty} \gamma + \Gamma(0, x^2) + \ln(x^2) = \infty$. Thus, the approximation Variant I given in Section 2.1 is not applicable, just as in the case of the $\boldsymbol{k} = \boldsymbol{0}$ term of the 2d-periodic Ewald sum. However, using the fast summation approach, the function is truncated and embedded in a smooth and periodic function, which does not require localization of the kernel function.

Similar as in the previous section we derive the fast algorithm based on (5.2) and (5.3). The evaluation of the short range part $\phi^{\mathrm{p1,S}}(\boldsymbol{x}_j)$ is done by a direct evaluation again. Due to Lemma 5.2 in[40] we truncate the infinite sum in $\phi^{\mathrm{p1,L}}(\boldsymbol{x}_j)$, i.e., for some appropriate $M_1 \in 2\mathbb{N}$ we set

$$\phi^{\mathrm{p1,L}}(\boldsymbol{x}_j) \approx \frac{2}{L} \sum_{k \in \mathcal{I}_{M_1} \backslash \{0\}} \sum_{i=1}^{N} q_i \mathrm{e}^{2\pi \mathrm{i}k x_{ij,1}/L}\Theta^{\mathrm{p1}}(k, \|\tilde{\boldsymbol{x}}_{ij}\|).$$

In the following we assume that $\tilde{\boldsymbol{x}}_j \in [-L_2/2, L_2/2] \times [-L_3/2, L_3/2]$, i.e., $\tilde{\boldsymbol{x}}_{ij} \in [-L_2, L_2] \times [-L_3, L_3]$. Thus, the particle distances regarding the non-periodic dimensions $\|\tilde{\boldsymbol{x}}_{ij}\|$ are bounded above by $\sqrt{L_2^2 + L_3^2}$. Furthermore, we choose some $h > 2\sqrt{L_2^2 + L_3^2}$ and accordingly some $\varepsilon \in (0, 1/2)$ such that $\|\tilde{\boldsymbol{x}}_{ij}\| \leq \sqrt{L_2^2 + L_3^2} =: h(1/2 - \varepsilon) < h/2$ for all $i, j = 1, \ldots, N$.

In order to approximate the long range part $\phi^{\mathrm{p1,L}}(\boldsymbol{x}_j) + \phi^{\mathrm{p1,0}}(\boldsymbol{x}_j)$ efficiently we consider for $k \in \{0, \ldots, {}^{M_1}\!/{}_2\}$ the regularizations

$$
K_{\mathrm{R}}(k,r) := \begin{cases}
\dfrac{2}{L}\Theta^{\mathrm{p1}}(k,r) & : k \neq 0, |h^{-1}r| \leq {}^{1}\!/{}_2 - \varepsilon, \\[2mm]
-\dfrac{1}{L}\Theta_0^{\mathrm{p1}}(r) & : k = 0, |h^{-1}r| \leq {}^{1}\!/{}_2 - \varepsilon, \\[2mm]
K_{\mathrm{B}}(k,r) & : |h^{-1}r| \in ({}^{1}\!/{}_2 - \varepsilon, {}^{1}\!/{}_2], \\[1mm]
K_{\mathrm{B}}(k,{}^{h}\!/{}_2) & : |h^{-1}r| > {}^{1}\!/{}_2,
\end{cases}
$$

where each function $K_{\mathrm{B}}(k,\cdot) : [{}^{h}\!/{}_2 - h\varepsilon, {}^{h}\!/{}_2] \to \mathbb{R}$ is constructed such that $K_{\mathrm{R}}(k, \|\cdot\|) : h\mathbb{T}^2 \to \mathbb{R}$ is in the Sobolev space $\mathrm{C}^{p-1}(h\mathbb{T}^2)$, i.e., $K_{\mathrm{B}}(k,\cdot)$ fulfills the interpolation conditions

$$
\frac{\partial^j}{\partial r^j} K_{\mathrm{B}}(k, {}^{h}\!/{}_2 - h\varepsilon) = \begin{cases}
\frac{2}{L}\frac{\partial^j}{\partial r^j}\Theta^{\mathrm{p1}}(k, {}^{h}\!/{}_2 - h\varepsilon) & : k \neq 0, \\[2mm]
-\frac{1}{L}\frac{\mathrm{d}^j}{\mathrm{d}r^j}\Theta_0^{\mathrm{p1}}({}^{h}\!/{}_2 - h\varepsilon) & : k = 0
\end{cases}
\tag{5.4}
$$

for $j = 0, \ldots, p - 1$ as well as

$$
\frac{\partial^j}{\partial r^j} K_{\mathrm{B}}(k, {}^{h}\!/{}_2) = 0 \quad \text{for } j = 1, \ldots, p - 1.
\tag{5.5}
$$

Note that $K_{\mathrm{R}}(k, \|\cdot\|)$ is constant for all the points $\{\boldsymbol{y} \in h\mathbb{T}^2 : \|\boldsymbol{y}\| \geq {}^{h}\!/{}_2\}$. Therefore, the conditions (5.5) ensure smoothness of $K_{\mathrm{R}}(k, \|\cdot\|)$ in the points $\{\boldsymbol{y} \in h\mathbb{T}^2 : \|\boldsymbol{y}\| = {}^{h}\!/{}_2\}$. Furthermore, (5.5) does not include any restriction on the function value of $K_{\mathrm{R}}(k,{}^{h}\!/{}_2)$, since it does not influence the smoothness of $K_{\mathrm{R}}(k, \|\cdot\|)$. In Appendix C of[40] we show that an adopted version of Theorem 2.1 can be used to construct the regularizing functions $K_{\mathrm{B}}(k, \|.\|)$ as interpolation polynomials of degree $2p-2$. By our construction the functions $K_{\mathrm{R}}(k, \|\cdot\|)$ are h-periodic in each direction and smooth, i.e., $K_{\mathrm{R}}(k, \|\cdot\|) \in \mathrm{C}^{p-1}(h\mathbb{T}^2)$. For a graphical illustration of a regularization $K_{\mathrm{R}}(k,\cdot)$ see Figure 5.1.

To this end, we approximate for each $k \in \mathcal{I}_{M_1} \setminus \{0\}$ the function

$$
\frac{2}{L}\Theta^{\mathrm{p1}}(k, \|\boldsymbol{y}\|) \approx \sum_{\boldsymbol{l} \in \mathcal{I}_{\tilde{\boldsymbol{M}}}} \hat{b}_{k,\boldsymbol{l}} \mathrm{e}^{2\pi \mathrm{i} \boldsymbol{l} \cdot \boldsymbol{y}/h}
\tag{5.6}
$$

for $\|\boldsymbol{y}\| \leq {}^{h}\!/{}_2 - h\varepsilon$ by a trigonometric polynomial. In the case $k = 0$ we use the approximation

$$
-\frac{1}{L}\Theta_0^{\mathrm{p1}}(\alpha^2 \|\boldsymbol{y}\|^2) \approx \sum_{\boldsymbol{l} \in \mathcal{I}_{\tilde{\boldsymbol{M}}}} \hat{b}_{0,\boldsymbol{l}} \mathrm{e}^{2\pi \mathrm{i} \boldsymbol{l} \cdot \boldsymbol{y}/h}.
\tag{5.7}
$$

Thereby, we choose $\tilde{\boldsymbol{M}} = (M_2, M_3) \in 2\mathbb{N}^2$ large enough and compute the Fourier coefficients $\hat{b}_{k,\boldsymbol{l}}$ by

$$
\hat{b}_{k,\boldsymbol{l}} := \frac{1}{|\mathcal{I}_{\tilde{\boldsymbol{M}}}|} \sum_{\boldsymbol{j} \in \mathcal{I}_{\tilde{\boldsymbol{M}}}} K_{\mathrm{R}}\left(k, \|\boldsymbol{j} \odot \tilde{\boldsymbol{M}}^{-1}\|h\right) \mathrm{e}^{-2\pi \mathrm{i} \boldsymbol{j} \cdot (\boldsymbol{l} \odot \tilde{\boldsymbol{M}}^{-1})}
$$

for all $k \in \mathcal{I}_{M_1}$.

For relatively large values of k we may again obtain a good approximation by setting

$$
\Theta^{\mathrm{p1}}(k, \|\boldsymbol{y}\|) \approx \sum_{\boldsymbol{n} \in \mathbb{Z}^2} \Theta^{\mathrm{p1}}(k, \|\boldsymbol{y} + h\boldsymbol{n}\|),
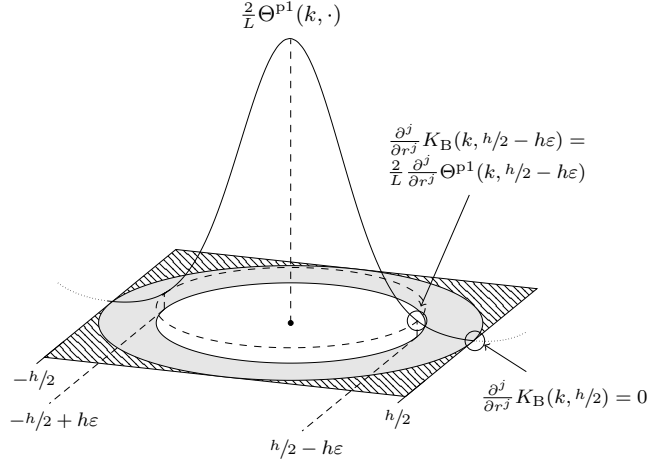$$

Figure 5.1. Example for $K_R(k, \cdot)$ for $k \geq 1$. Over the gray area the regularization adopts the values of the boundary function $K_B(k, \cdot)$, which we compute via a modified two point Taylor interpolation. In the corners (striped area) $K_R(k, \cdot)$ has the constant value $K_B(k, h/2)$. We also marked the points, where the conditions (5.4) and (5.5) are fulfilled.

compare to the 2d-periodic case and Figure 4.2. With the help of the analytical Fourier transform

$$\hat{\Theta}^{P1}(k, \|\boldsymbol{\xi}\|) = \frac{L^2}{2\pi(k^2 + L^2\|\boldsymbol{\xi}\|^2)} e^{-\pi^2 k^2/(\alpha^2 L^2) - \pi^2\|\boldsymbol{\xi}\|^2/\alpha^2}$$

and the Poisson summation formula we get

$$\frac{2}{L}\hat{\Theta}^{P1}(k, \|\boldsymbol{y}\|) \approx \frac{2}{L} \sum_{\boldsymbol{n} \in \mathbb{Z}^2} \Theta^{P1}(k, \|\boldsymbol{y} + h\boldsymbol{n}\|) \approx \frac{2}{Lh^2} \sum_{\boldsymbol{l} \in \mathcal{I}_{\tilde{M}}} \hat{\Theta}^{P1}(k, h^{-1}\|\boldsymbol{l}\|) e^{2\pi i \boldsymbol{l} \cdot \boldsymbol{y}/h},$$

i.e., we can simply set $\hat{b}_{k,\boldsymbol{l}} := 2(Lh^2)^{-1}\hat{\Theta}^{P1}(k, h^{-1}\|\boldsymbol{l}\|)$ instead of regularizing the function.

In summary we obtain the following approximation for the long range parts

$$\phi^{P1,L}(\boldsymbol{x}_j) + \phi^{P1,0}(\boldsymbol{x}_j) \approx \sum_{k \in \mathcal{I}_{M_1}} \sum_{\boldsymbol{l} \in \mathcal{I}_{\tilde{M}}} \hat{b}_{|k|,\boldsymbol{l}} \sum_{i=1}^{N} q_i e^{2\pi i k x_{ij,1}/L} e^{2\pi i \boldsymbol{l} \cdot \tilde{\boldsymbol{x}}_{ij}/h}$$

$$= \sum_{(k,\boldsymbol{l}) \in \mathcal{I}_{\boldsymbol{M}}} \hat{b}_{|k|,\boldsymbol{l}} \left(\sum_{i=1}^{N} q_i e^{2\pi i \boldsymbol{v}(k,\boldsymbol{l}) \cdot \boldsymbol{x}_i} \right) e^{-2\pi i \boldsymbol{v}(k,\boldsymbol{l}) \cdot \boldsymbol{x}_j},$$

where we use the truncated Fourier series (5.6) and (5.7) and define $\boldsymbol{M} := (M_1, \tilde{\boldsymbol{M}}) \in 2\mathbb{N}^3$ as well as the vectors $\boldsymbol{v}(k, \boldsymbol{l}) := (k/L, \boldsymbol{l}/h) \in L^{-1}\mathbb{Z} \times h^{-1}\mathbb{Z}^2$.

The expressions in the inner brackets

$$\hat{S}(k, \boldsymbol{l}) := \sum_{i=1}^{N} q_i e^{2\pi i \boldsymbol{v}(k,\boldsymbol{l}) \cdot \boldsymbol{x}_i}, \quad (k, \boldsymbol{l}) \in \mathcal{I}_{\boldsymbol{M}},$$

17

can be computed by an adjoint NFFT. This will be followed by $|\mathcal{I}_{\boldsymbol{M}}|$ multiplications with $\hat{b}_{|k|,\boldsymbol{l}}$ and completed by an NFFT to compute the outer summation over the indexes $(k, \boldsymbol{l}) \in \mathcal{I}_{\boldsymbol{M}}$. The proposed evaluation of $\phi^{\mathrm{p1,L}}(\boldsymbol{x}_j) + \phi^{\mathrm{p1,0}}(\boldsymbol{x}_j)$ at the points $\boldsymbol{x}_j$, $j = 1, \ldots, N$, requires $\mathcal{O}(N + |\mathcal{I}_{\boldsymbol{M}}| \log |\mathcal{I}_{\boldsymbol{M}}|)$ arithmetic operations.

Again, using a matrix-vector notation we can write

$$\left(\phi^{\mathrm{p1,L}}(\boldsymbol{x}_j) + \phi^{\mathrm{p1,0}}(\boldsymbol{x}_j)\right)_{j=1}^{N} \approx \tilde{\boldsymbol{A}} \boldsymbol{D} \tilde{\boldsymbol{A}}^{\mathsf{H}} \boldsymbol{q}, \tag{5.8}$$

where $\tilde{\boldsymbol{A}}$ denotes the matrix representation of the NFFT in three dimensions for the nodes $(x_{j,1}/L, \tilde{\boldsymbol{x}}_j/h) \in \mathbb{T}^3$, $\boldsymbol{D}$ is a diagonal matrix with entries $\hat{b}_{|k|,\boldsymbol{l}}$, $(k, \boldsymbol{l}) \in \mathcal{I}_{\boldsymbol{M}}$, and $\boldsymbol{q} = (q_1, \ldots, q_N)^{\top} \in \mathbb{R}^N$.

Relations to existing work

The Ewald formulas for 1d-periodic geometries were already proposed in[46]. Some Fourier based algorithms, like MMM1D[7], where already proposed. A method based on approximation Variant II from Section 2.1 is proposed in[36]. However, as mentioned in Section 2.1 this method suffers from the rather slow convergence rate in Fourier space. See also[53, 10] for algorithms with higher complexity.

6 Fast Ewald summation for 0d-periodic (open) boundary conditions

We consider a (not necessarily electrical neutral) system of N charges $q_j \in \mathbb{R}$ at positions $\boldsymbol{x}_j \in \mathbb{R}^3$, $j = 1, \ldots, N$. Under open boundary conditions the potential of each single particle j is defined by

$$\phi^{\mathrm{p0}}(\boldsymbol{x}_j) := \phi_{\{0\}^3}(\boldsymbol{x}_j) = \sum_{i=1}^{N}{}' \frac{q_i}{\|\boldsymbol{x}_{ij}\|},$$

i.e., we set $\mathcal{S} := \{0\}^3$ within the definition (1.3). This can be rewritten as

$$\phi^{\mathrm{p0}}(\boldsymbol{x}_j) = \phi^{\mathrm{p0,S}}(\boldsymbol{x}_j) + \phi^{\mathrm{p0,L}}(\boldsymbol{x}_j) + \phi^{\mathrm{p0,self}}(\boldsymbol{x}_j),$$

where for the splitting parameter $\alpha > 0$ we define the short range part

$$\phi^{\mathrm{p0,S}}(\boldsymbol{x}_j) := \sum_{i=1}^{N}{}' q_i \frac{\mathrm{erfc}(\alpha\|\boldsymbol{x}_{ij}\|)}{\|\boldsymbol{x}_{ij}\|},$$

the long range part

$$\phi^{\mathrm{p0,L}}(\boldsymbol{x}_j) := \sum_{i=1}^{N} q_i \Theta^{\mathrm{p0}}(\|\boldsymbol{x}_{ij}\|), \tag{6.1}$$

the self potential

$$\phi^{\mathrm{p0,self}}(\boldsymbol{x}_j) := -\frac{2\alpha}{\sqrt{\pi}} q_j,$$

and the function $\Theta^{\mathrm{P0}}(r)$ is defined by

$$\Theta^{\mathrm{P0}}(r) = \begin{cases} \frac{2\alpha}{\sqrt{\pi}} & : r = 0, \\ \frac{\mathrm{erf}(\alpha r)}{r} & : \text{else.} \end{cases}$$

Using Variant III of Section 2, i.e., the fast summation approach, the function is approximated by a Fourier series. Similar as in the previous section we derive the fast algorithm now based on (6.1). The evaluation of the short range part $\phi^{\mathrm{P0,S}}(\boldsymbol{x}_j)$ is done by a direct evaluation again.

In the following we assume that we have $\|\boldsymbol{x}_{ij}\| \leq L =: h(1/2 - \varepsilon)$. As an example, if $\boldsymbol{x}_j \in L_1\mathbb{T} \times L_2\mathbb{T} \times L_3\mathbb{T}$, we can set $L := \sqrt{L_1^2 + L_2^2 + L_3^2}$. In order to approximate the long range part $\phi^{\mathrm{P0,L}}(\boldsymbol{x}_j)$ efficiently we consider the regularizations

$$K_{\mathrm{R}}(r) := \begin{cases} \Theta^{\mathrm{P0}}(r) & : |h^{-1}r| \leq 1/2 - \varepsilon, \\ K_{\mathrm{B}}(r) & : |h^{-1}r| \in (1/2 - \varepsilon, 1/2], , \\ K_{\mathrm{B}}(h/2) & : |h^{-1}r| > 1/2, \end{cases}$$

where the function $K_{\mathrm{B}}(\cdot) : [h/2 - h\varepsilon, h/2] \to \mathbb{R}$ is constructed such that $K_{\mathrm{R}}(\|\cdot\|) : h\mathbb{T}^3 \to \mathbb{R}$ is in the Sobolev space $\mathrm{C}^{p-1}(h\mathbb{T}^3)$, i.e., $K_{\mathrm{B}}(k, \cdot)$ fulfills the interpolation conditions

$$\frac{\mathrm{d}^j}{\mathrm{d}r^j}K_{\mathrm{B}}(h/2 - h\varepsilon) = \frac{\mathrm{d}^j}{\mathrm{d}r^j}\Theta^{\mathrm{P0}}(h/2 - h\varepsilon) \quad \text{for } j = 0, \ldots, p-1$$

as well as

$$\frac{\mathrm{d}^j}{\mathrm{d}r^j}K_{\mathrm{B}}(h/2) = 0 \quad \text{for } j = 1, \ldots, p-1. \tag{6.2}$$

Note that $K_{\mathrm{R}}(\|\cdot\|)$ is constant for all the points $\{\boldsymbol{y} \in h\mathbb{T}^3 : \|\boldsymbol{y}\| \geq h/2\}$. Therefore, the conditions (6.2) ensure smoothness of $K_{\mathrm{R}}(\|\cdot\|)$ in the points $\{\boldsymbol{y} \in h\mathbb{T}^3 : \|\boldsymbol{y}\| = h/2\}$. Furthermore, (6.2) does not include any restriction on the function value of $K_{\mathrm{R}}(h/2)$, since it does not influence the smoothness of $K_{\mathrm{R}}(\|\cdot\|)$. In Appendix C of[40] we show that an adopted version of Theorem 2.1 can be used to construct the regularizing functions $K_{\mathrm{B}}(k, \|.\|)$ as interpolation polynomials of degree $2p-2$. By our construction the function $K_{\mathrm{R}}(\|\cdot\|)$ is h-periodic in each direction and smooth, i.e., $K_{\mathrm{R}}(\|\cdot\|) \in \mathrm{C}^{p-1}(h\mathbb{T}^3)$.

To this end, we approximate the function

$$\Theta^{\mathrm{P0}}(\|\boldsymbol{y}\|) \approx \sum_{\boldsymbol{l}\in\mathcal{I}_M} \hat{b}_{\boldsymbol{l}} \mathrm{e}^{2\pi\mathrm{i}\boldsymbol{l}\cdot\boldsymbol{y}/h}$$

for $\|\boldsymbol{y}\| \leq h/2 - h\varepsilon$ by a trigonometric polynomial. Thereby, we choose $\boldsymbol{M} = (M_1, M_2, M_3) \in 2\mathbb{N}^2$ large enough and compute the Fourier coefficients $\hat{b}_{\boldsymbol{l}}$ by

$$\hat{b}_{\boldsymbol{l}} := \frac{1}{|\mathcal{I}_{\boldsymbol{M}}|} \sum_{\boldsymbol{j}\in\mathcal{I}_{\boldsymbol{M}}} K_{\mathrm{R}}\left(\|\boldsymbol{j}\odot\boldsymbol{M}^{-1}\|h\right) \mathrm{e}^{-2\pi\mathrm{i}\boldsymbol{j}\cdot(\boldsymbol{l}\odot\boldsymbol{M}^{-1})}.$$

In summary we obtain the following approximation for the long range parts

$$\phi^{\mathrm{P0,L}}(\boldsymbol{x}_j) \approx \sum_{\boldsymbol{l}\in\mathcal{I}_M} \hat{b}_{\boldsymbol{l}} \sum_{i=1}^{N} q_i \mathrm{e}^{2\pi\mathrm{i}\boldsymbol{l}\cdot\boldsymbol{x}_{ij}/h}$$

$$= \sum_{\boldsymbol{l}\in\mathcal{I}_M} \hat{b}_{\boldsymbol{l}} \left(\sum_{i=1}^{N} q_i \mathrm{e}^{2\pi\mathrm{i}\boldsymbol{l}\cdot\boldsymbol{x}_i/h}\right) \mathrm{e}^{-2\pi\mathrm{i}\boldsymbol{l}\cdot\boldsymbol{x}_j/h},$$

where we use the truncated Fourier series. The expressions in the inner brackets

$$\hat{S}(\boldsymbol{l}) := \sum_{i=1}^{N} q_i \mathrm{e}^{2\pi \mathrm{i} \boldsymbol{l} \cdot \boldsymbol{x}_i / h}, \quad \boldsymbol{l} \in \mathcal{I}_{\boldsymbol{M}},$$

can be computed by an adjoint NFFT. This will be followed by $|\mathcal{I}_{\boldsymbol{M}}|$ multiplications with $\hat{b}_l$ and completed by an NFFT to compute the outer summation with the complex exponentials. The proposed evaluation of $\phi^{\mathrm{p1,L}}(\boldsymbol{x}_j) + \phi^{\mathrm{p1,0}}(\boldsymbol{x}_j)$ at the points $\boldsymbol{x}_j$, $j = 1, \ldots, N$, requires $\mathcal{O}(N + |\mathcal{I}_{\boldsymbol{M}}| \log |\mathcal{I}_{\boldsymbol{M}}|)$ arithmetic operations.

As for the different types of periodic boundary conditions, we also obtain a matrix-vector notation for the 0d-periodic case, which reads as

$$\left(\phi^{\mathrm{p0,L}}(\boldsymbol{x}_j)\right)_{j=1}^{N} \approx \tilde{\boldsymbol{A}} \boldsymbol{D} \tilde{\boldsymbol{A}}^{\mathsf{H}} \boldsymbol{q}, \tag{6.3}$$

where $\tilde{\boldsymbol{A}}$ denotes the matrix representation of the NFFT in three dimensions for the nodes $\boldsymbol{x}_j / h \in \mathbb{T}^3$, $\boldsymbol{D}$ is a diagonal matrix with entries $\hat{b}_l$, $\boldsymbol{l} \in \mathcal{I}_{\boldsymbol{M}}$, and $\boldsymbol{q} = (q_1, \ldots, q_N)^{\top} \in \mathbb{R}^N$.

Relations to existing work

This method can be interpreted as nonequispaced convolution. For equispaced nodes the discrete convolution and its fast computation is typically realized by FFT exploiting the basic property $\mathrm{e}^{2\pi \mathrm{i}(y-x)} = \mathrm{e}^{2\pi \mathrm{i} y} \mathrm{e}^{-2\pi \mathrm{i} x}$. Following these lines, the method can be interpreted as "convolution at nonequispaced nodes" by Fourier methods as well, more precisely by the NFFT. This new method includes convolutions, e.g., with kernels of the form $1/\|x\|$. We remark that some FFT-accelerated Ewald[26, 22] methods contain similar steps as the fast summation based on NFFT. A method based on approximation Variant II from Section 2.1 is proposed in[37]. However, as mentioned in Section 2.1 this method suffers from the rather slow convergence rate in Fourier space.

7 Conclusion

With this tutorial we provide an overview of the NFFT based fast Ewald summation for all kinds of mixed periodic boundary conditions. The main advantage of our approach is that all presented algorithms have a common structure. More precisely, the short range parts of the potentials are always computed directly and the long range parts are computed by an adjoint NFFT, a point-wise multiplication in Fourier space and, again, an NFFT in three dimensions, see the matrix vector notation for the 3d-periodic case in (3.2), for the 2d-periodic case in (4.8), for the 1d-periodic case in (5.8), and for the 0d-periodic case in (6.3). Non-periodic boundary conditions are handled via a combination of the corresponding mixed-periodic Ewald formulas and the concept of NFFT based fast summation. Thereby, we embed the non-periodic functions of the mixed-periodic Ewald formulas into smooth periodic functions and obtain rapidly convergent Fourier approximations. Note that this approach also includes the 0d-periodic (open) case.

Since all algorithms depend on common building blocks, code and algorithm improvements can be realized individually on the more elementary submodules. For example, a MPI-based parallel NFFT algorithm was proposed in[45] and is publicly available[42]. The

parallelization of the NFFT module led to a parallel version of all the above mentioned Ewald summation methods at once.

Following the naming scheme of the particle-particle particle-mesh (P^3M) method, our proposed framework is called particle-particle NFFT (P^2NFFT), since the short range particle-particle interactions are computed in the same way as in P^3M algorithms, while the long range particle-mesh part is computed by NFFTs.

In order to rate the very good performance of the proposed algorithms, we compared the method to the P^2NFFT method for 3d-periodic systems[45] as well as to the method proposed in[34] by considering similar numerical examples, see[40]. Note that the P^2NFFT algorithm is highly optimized, publicly available[5], and recently compared to other methods, such as the P^3M method, the fast multipole method and multigrid based methods, see[4] and the references therein.

Acknowledgments

References

1. M. Abramowitz and I. A. Stegun, editors. *Handbook of Mathematical Functions*. National Bureau of Standards, Washington, DC, USA, 1972.

2. R. P. Agarwal and P. J. Y. Wong. *Error inequalities in polynomial interpolation and their applications*, volume 262 of *Mathematics and its Applications*. Kluwer Academic Publishers Group, Dordrecht, 1993.

3. A. Arnold, J. de Joannis, and C. Holm. Electrostatics in periodic slab geometries. I. *J. Chem. Phys.*, 117:2496, 2002.

4. A. Arnold, F. Fahrenberger, C. Holm, O. Lenz, M. Bolten, H. Dachsel, R. Halver, I. Kabadshow, F. Gähler, F. Heber, J. Iseringhausen, M. Hofmann, M. Pippig, D. Potts, and G. Sutmann. Comparison of scalable fast methods for long-range interactions. *Phys. Rev. E*, 88:063308, 2013.

5. A. Arnold, F. Fahrenberger, O. Lenz, M. Bolten, H. Dachsel, R. Halver, I. Kabadshow, F. Gähler, F. Heber, J. Iseringhausen, M. Hofmann, and M. Pippig. ScaFaCoS - Scalable Fast Coloumb Solvers. http://www.scafacos.de.

6. A. Arnold and C. Holm. MMM2D: A fast and accurate summation method for electrostatic interactions in 2D slab geometries. *Comput. Phys. Commun.*, 148:327 – 348, 2002.

7. A. Arnold and C. Holm. MMM1D: A method for calculating electrostatic interactions in one-dimensional periodic geometries. *J. Chem. Phys.*, 123:144103, 2005.

8. G. Beylkin. On the fast Fourier transform of functions with singularities. *Appl. Comput. Harmon. Anal.*, 2:363 – 381, 1995.

9. A. Bródka. Ewald summation method with electrostatic layer correction for interactions of point dipoles in slab geometry. *Chem. Phys. Lett.*, 400:62 – 67, 2004.

10. A. Bródka and P. Sliwinski. Three-dimensional Ewald method with correction term for a system periodic in one direction. *J. Chem. Phys.*, 120:5518 – 5523, 2004.

11. T. Darden, D. York, and L. Pedersen. Particle mesh Ewald: An $N \log(N)$ method for Ewald sums in large systems. *J. Chem. Phys.*, 98:10089–10092, 1993.

12. S. W. de Leeuw, J. W. Perram, and E. R. Smith. Simulation of electrostatic systems in periodic boundary conditions. I. Lattice sums and dielectric constants. *Proc. Roy. Soc. London Ser. A*, 373:27 – 56, 1980.

13. M. Deserno and C. Holm. How to mesh up Ewald sums. I. A theoretical and numerical comparison of various particle mesh routines. *J. Chem. Phys.*, 109:7678 – 7693, 1998.

14. A. Dutt and V. Rokhlin. Fast Fourier transforms for nonequispaced data. *SIAM J. Sci. Stat. Comput.*, 14:1368 – 1393, 1993.

15. U. Essmann, L. Perera, M. L. Berkowitz, T. Darden, H. Lee, and L. G. Pedersen. A smooth particle mesh Ewald method. *J. Chem. Phys.*, 103:8577 – 8593, 1995.

16. P. P. Ewald. Die Berechnung optischer und elektrostatischer Gitterpotentiale. *Ann. Phys.*, 369:253–287, 1921.

17. M. Fenn and G. Steidl. Fast NFFT based summation of radial functions. *Sampl. Theory Signal Image Process.*, 3:1 – 28, 2004.

18. J. A. Fessler and B. P. Sutton. Nonuniform fast Fourier transforms using min-max interpolation. *IEEE Trans. Signal Process.*, 51:560 – 574, 2003.

19. D. Frenkel and B. Smit. *Understanding molecular simulation: From algorithms to applications*. Academic Press, 2002.

20. M. Frigo and S. G. Johnson. FFTW, C subroutine library. http://www.fftw.org, 2009.

21. L. Greengard and J.-Y. Lee. Accelerating the nonuniform fast Fourier transform. *SIAM Rev.*, 46:443 – 454, 2004.

22. M. Griebel, S. Knapek, and G. Zumbusch. *Numerical simulation in molecular dynamics*, volume 5 of *Texts in Computational Science and Engineering*. Springer, Berlin, 2007.

23. A. Grzybowski, E. Gwóźdź, and A. Bródka. Ewald summation of electrostatic interactions in molecular dynamics of a three-dimensional system with periodicity in two directions. *Phys. Rev. B*, 61:6706–6712, 2000.

24. F. E. Harris. Incomplete Bessel, generalized incomplete gamma, or leaky aquifer functions. *J. Comput. Appl. Math.*, 215:260 – 269, 2008.

25. F. Hedman and A. Laaksonen. Ewald summation based on nonuniform fast Fourier transform. *Chem. Phys. Lett.*, 425:142 – 147, 2006.

26. R. W. Hockney and J. W. Eastwood. *Computer simulation using particles*. Taylor & Francis, Inc., Bristol, PA, USA, 1988.

27. P. H. Hünenberger. Lattice-sum methods for computing electrostatic interactions in molecular simulations. In *Simulation and theory of electrostatic interactions in solution*, volume 17, pages 17 – 83. ASCE, 1999.

28. D. Huybrechs. On the Fourier extension of nonperiodic functions. *SIAM J. Numer. Anal.*, 47(6):4326 – 4355, 2010.

29. J. Keiner, S. Kunis, and D. Potts. NFFT 3.0, C subroutine library. http://www.tu-chemnitz.de/~potts/nfft.

30. J. Keiner, S. Kunis, and D. Potts. Using NFFT3 - a software library for various nonequispaced fast Fourier transforms. *ACM Trans. Math. Software*, 36:Article 19, 1 – 30, 2009.

31. S. Kunis and S. Kunis. The nonequispaced FFT on graphics processing units. *PAMM, Proc. Appl. Math. Mech.*, 12, 2012.

32. S. Kunis and D. Potts. Time and memory requirements of the nonequispaced FFT. *Sampl. Theory Signal Image Process.*, 7:77 – 100, 2008.

33. D. Lindbo and A.-K. Tornberg. Spectral accuracy in fast Ewald-based methods for particle simulations. *J. Comput. Phys.*, 230:8744 – 8761, 2011.

34. D. Lindbo and A.-K. Tornberg. Fast and spectrally accurate Ewald summation for 2-periodic electrostatic systems. *J. Chem. Phys.*, 136:164111, 2012.

35. M. Lyon. Approximation error in regularized SVD-based Fourier continuations. *Appl. Numer. Math.*, 62(12):1790 – 1803, 2012.

36. P. Minary, J. A. Morrone, D. A. Yarne, M. E. Tuckerman, and G. J. Martyna. Long range interactions on wires: a reciprocal space based formalism. *J. Chem. Phys.*, 121:11949 – 11956, 2004.

37. P. Minary and M. E. Tuckerman. A reciprocal space based method for treating long range interactions in ab initio and force-field-based calculations in clusters. *J. Chem. Phys.*, 110:2810 – 2821, 1999.

38. P. Minary, M. E. Tuckerman, K. A. Pihakari, and G. J. Martyna. A new reciprocal space based treatment of long range interactions on surfaces. *J. Chem. Phys.*, 116:5351 – 5362, 2002.

39. F. Nestler. Automated parameter tuning based on RMS errors for nonequispaced FFTs. *Preprint 2015-01, Faculty of Mathematics, Technische Universität Chemnitz*, 2015.

40. F. Nestler, M. Pippig, and D. Potts. Fast Ewald summation based on NFFT with mixed periodicity. *J. Comput. Phys.*, 285:280 – 315, 2015.

41. M. Pippig. PFFT, Parallel FFT subroutine library. http://www.tu-chemnitz.de/~mpip/software.php, 2011.

42. M. Pippig. PNFFT, Parallel Nonequispaced FFT subroutine library. http://www.tu-chemnitz.de/~mpip/software.php, 2011.

43. M. Pippig. PFFT - An extension of FFTW to massively parallel architectures. *SIAM J. Sci. Comput.*, 35:C213 – C236, 2013.

44. M. Pippig and D. Potts. Particle simulation based on nonequispaced fast Fourier transforms. In G. Sutmann, P. Gibbon, and T. Lippert, editors, *Fast Methods for Long-Range Interactions in Complex Systems*, volume 6 of *IAS-Series*, pages 131 – 158, Jülich, 2011. Forschungszentrum Jülich GmbH.

45. M. Pippig and D. Potts. Parallel three-dimensional nonequispaced fast Fourier transforms and their application to particle simulation. *SIAM J. Sci. Comput.*, 35:C411 – C437, 2013.

46. M. Porto. Ewald summation of electrostatic interactions of systems with finite extent in two of three dimensions. *J. Phys. A*, 33:6211 – 6218, 2000.

47. D. Potts and G. Steidl. Fast summation at nonequispaced knots by NFFTs. *SIAM J. Sci. Comput.*, 24:2013 – 2037, 2003.

48. D. Potts, G. Steidl, and M. Tasche. Fast Fourier transforms for nonequispaced data: A tutorial. In J. J. Benedetto and P. J. S. G. Ferreira, editors, *Modern Sampling Theory: Mathematics and Applications*, pages 247 – 270, Boston, MA, USA, 2001. Birkhäuser.

49. G. Steidl. A note on fast Fourier transforms for nonequispaced grids. *Adv. Comput.*

Math., 9:337 – 353, 1998.

50. T. Volkmer. OpenMP parallelization in the NFFT software library. *Preprint TU Chemnitz*, Preprint 7, 2012.

51. Y.-L. Wang, F. Hedman, M. Porcu, F. Mocci, and A. Laaksonen. Non-uniform FFT and its applications in particle simulations. *App. Math.*, 5:520 – 541, 2014.

52. A. H. Widmann and D. B. Adolf. A comparison of Ewald summation techniques for planar surfaces. *Comput. Phys. Commun.*, 107:167 – 186, 1997.

53. I.-C. Yeh and M. L. Berkowitz. Ewald summation for systems with slab geometry. *J. Chem. Phys.*, 111(7):3155 – 3162, 1999.